Select-Low and Select-High Methods for the Wheeled Robot Dynamic States Control

Bogusław Schreyer

***Abstract*—**The paper enquires on the two methods of the wheeled robot braking torque control. Those two methods are applied when the adhesion coefficient under left side wheels is different from the adhesion coefficient under the right side wheels. In case of the select-low (SL) method the braking torque on both wheels is controlled by the signals originating from the wheels on the side of the lower adhesion. In the select-high (SH) method the torque is controlled by the signals originating from the wheels on the side of the higher adhesion. The SL method is securing stable and secure robot behaviors during the braking process. However, the efficiency of this method is relatively low. The SH method is more efficient in terms of time and braking distance but in some situations may cause wheels blocking. It is important to monitor the velocity of all wheels and then take a decision about the braking torque distribution accordingly. In case of the SH method the braking torque slope may require significant decrease in order to avoid wheel blocking.

***Keywords*—**Select-high method, select-low method, torque distribution, wheeled robot.

I. Introduction

THE general movement equations in 3 dimensions can be derived from the Lagrange equations [2], [3]:

$$\frac{d}{dt}\left(\frac{\partial K}{\partial \dot{q}}\right) - \frac{\partial K}{\partial q} + \frac{\partial F}{\partial \dot{q}} + \frac{\partial V}{\partial q} = Q \quad (1)$$

where K: total kinetic energy, F: dissipation function, V: potential energy, Q: generalized forces, $q\dot{}$: generalized coordinates and velocities,

$$K = K_r + K_n,$$

where K_r-kinetic energy of sprang mass, K_n-kinetic energy of unsprang mass.

$$K_r = \frac{1}{2}M_r(\dot{x}^2 + \dot{y}^2 + \dot{z}^2) + \frac{1}{2}I_{xr}p^2 + \frac{1}{2}I_{yr}q^2 + \frac{1}{2}I_{zr}r^2 - c_{xzr}\cdot r\cdot p,$$

where M_r- sprang mass, I_{xr}, I_{yr}, I_{zr}: sprang mass' moment of inertia relative to OX OY OZ, c_{xzr}: deviation moment of inertia relative to XZ plane. The corresponding system of coordinates is shown on Fig. 1.

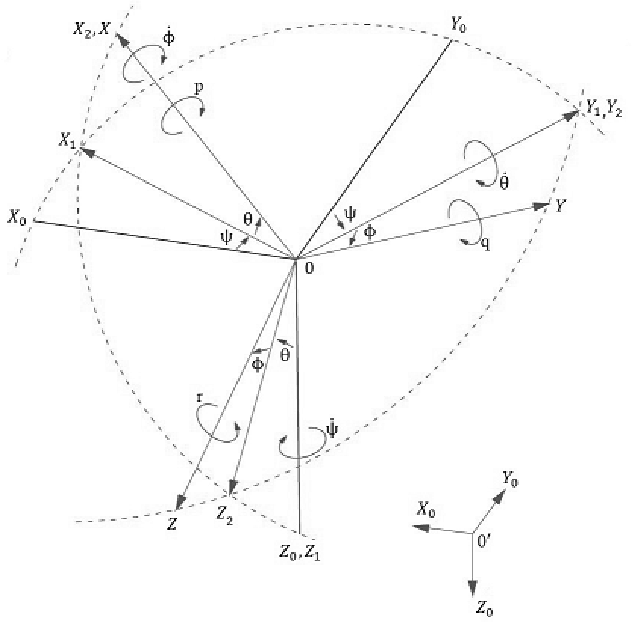

Fig. 1 System of Cartesian coordinates

II. Longitudinal Model Torque Control

The suspension in a wheeled robot can be neglected. Assuming also symmetry of the robot, the equations can be simplified.

The following are the robot's equations of motion while braking [4]:

$$M\dot{V} = -F_f \text{-} F_r = -N_f\mu_f - N_r\mu_r \quad (2)$$

where $\dot{V} = \frac{dV}{dt}$ and M is a total mass of a robot, μ_f and μ_r are the rear and front traction coefficients respectively. The dynamics of the front and rear wheels are described by:

$$I_f\dot{\omega}_f = F_fR_f - T_f \quad (3)$$

$$I_r\dot{\omega}_r = F_rR_r - T_r \quad (4)$$

where $\dot{\omega} = \frac{d\omega}{dt}$, ω is a wheel' rotational I is a wheel' moment of inertia, F is a friction force, R is a wheel' radius, T is a braking torque.

In order to secure optimum traction coefficients, both front and rear traction coefficients should be equal, for given slip value. Therefore, the both angular velocities must be equal: If $\mu_f = \mu_r = \mu$ then (2) becomes:

$$M\dot{V} = -\mu(N_f + N_r) \quad (6)$$

B.J. Schreyer is with Nipissing University, North Bay, Ontario, Canada (phone: 705 474 3450, e-mail: bjs@nipiossingu.ca).

And the slip value s, same for both – front and rear wheels, becomes

$$s = \frac{V-\omega R}{V} \tag{7}$$

From (6) we obtain:

$$\dot{\mu} = \frac{d\mu}{dt} = -\frac{\ddot{V}}{g} \tag{8}$$

where $\ddot{V}=\frac{d\dot{V}}{dt}$.

From (8) we obtain:

$$\dot{\mu} > 0 \leftrightarrow - \ddot{V} > 0 \tag{9}$$

In order to secure $\mu_f = \mu_r$, we need $\omega_f = \omega_r$, therefore $\dot{\omega}_f = \dot{\omega}r$. It can be shown, that in order to obtain $\mu_f = \mu_r$ we need to secure a correct value of T_f in function of T_r. Indeed, from (2)-(4) and (6) it can be deduced that [1]:

$$T_f = T_r - \frac{\dot{V}}{g} R\,(N_f - N_r) \tag{9}$$

Figs. 4 and 5 show the process of braking control assuming identical traction coefficient under all wheels. The robot model corresponding to such a symmetric traction coefficient is depicted on Fig. 2. This model allows for optimal (extremal) control of braking robot in aa variety of traction coefficients, as shown on Fig. 3. The friction coefficient graphs are symmetrical for braking and starting process. Figs. 4 and 5 show that the wheel sleep and wheel rotational velocity of all wheels are identical. The correct braking torque distribution ensures that the all slips and, at the same time, all traction coefficients are the same, therefore all wheels may reach the traction maxima at the same time. The rear torque is changing independently, while the front torque value satisfies (9).

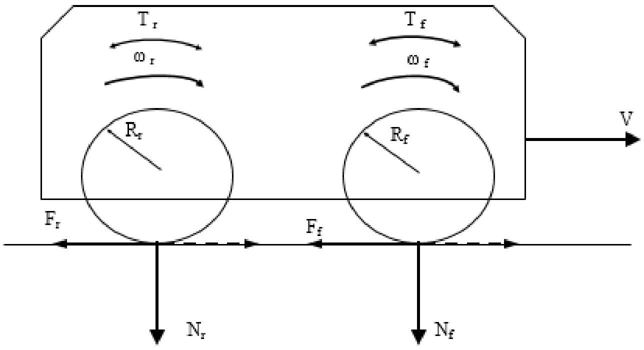

Fig. 2 Flat longitudinal robot model

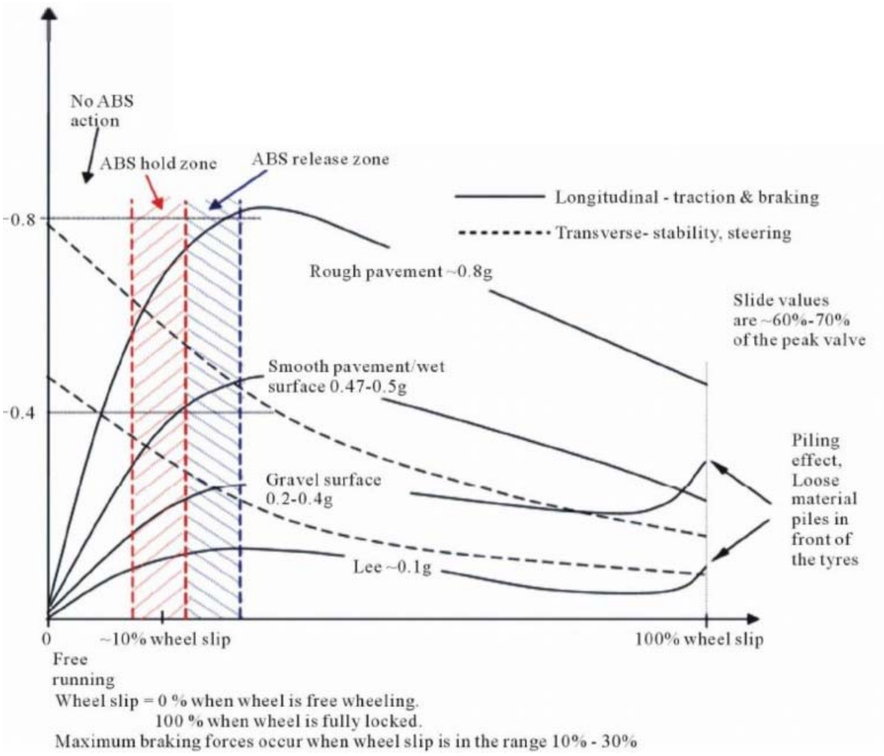

Fig. 3 Friction coefficients

III. Select-Low and Select-High Control

In practice, the anti-skid systems secure efficient and safe braking of the wheeled robot. They also ensure sufficient (although not perfect) transversal stability of the braking and the starting robot. The braking robot and wheel-road interaction are strongly nonlinear with parameters varying in function of linear speed of the robot, adhesion coefficient, weight and geometry of the vehicle, state of tires and random road and weather conditions. For these reasons, all existing systems are in fact quasi-optimal [8], [9]. On most road surfaces and under most weather conditions the road-wheel traction coefficient μ has its distinct maximum in function of the wheel slip s. The essence of the optimal and adaptive controller is to keep this adhesion near the maximum for all the wheels during the process of braking/starting. This simplified model is correct under all symmetry assumptions. When the asymmetry of traction coefficient between left and right wheels occurs, an anti-skid system should take a decision which friction coefficient will be taken as a reference: the lower or the higher one. In the first case we call it Select-Low method, in the second case we call it Select-High method, as suggested in [5].

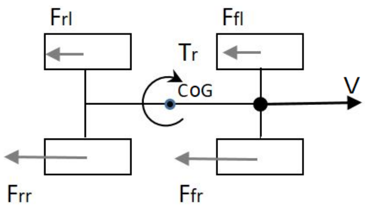

Fig. 4 Asymmetric traction coefficient

In case of asymmetric traction coefficient, the external forces applied to the tires are also asymmetric, i.e., the left front and rear braking forces Ffl and Frl are different from right side forces: Ffr and Frr. As a result, a rotational torque Tr is being generated. The rotational torque tends to rotate the robot. When the active transversal forces on a tire are bigger than the transversal friction forces, the tire tends to deform, and then to move transversally. The current model is not analyzing the transversal robot movement. When the active transversal force on any tire is bigger than then the transversal traction force, the braking moment is released.

In this paper a simplifying assumption has been introduced: it has been assumed that the left wheels are in the same road conditions, i.e., that the left front traction coefficient is equal the left rear: traction coefficient:

$$\mu_{fl}(s_l)=\mu_{rl}(s_l),$$

where s_l is a left wheels' slip:

$$s_l == \frac{V-\omega l * R}{V}$$

where ω_l is the left wheels (both of them) rotational velocity.

The same relation is true for the right wheels:

$$\mu_{fr}(s_r)=\mu_{rr}(s_r),$$

where s_r is a right wheels' slip:

$$s_r= \frac{V-\omega r * R}{V}$$

and ω_r is a right wheels (both of them) rotational velocity. In all formulas the v is a robot's linear velocity. In result, the active braking forces are:

$$Ffl=Nf\ \mu_{fl}$$
$$Frl=Nr\ \mu_{rl}$$
$$Ffr=Nf\ \mu_{fr}$$
$$Frr=Nr\ \mu_{rr}$$

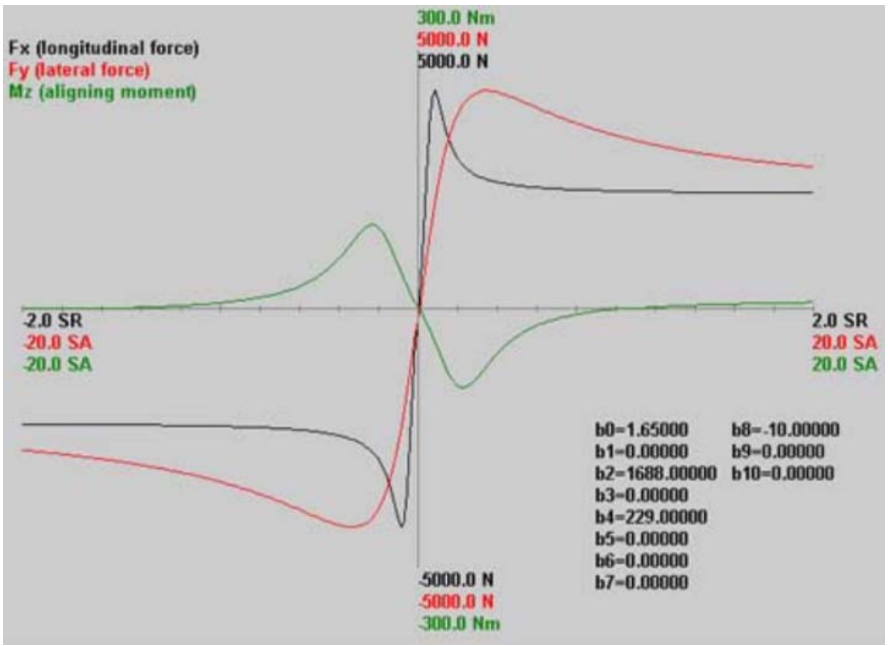

Fig. 5 Pacejka curves for transversal tire forces.

On Fig. 5 [7], [10] the black line indicates Fx (longitudinal, a result from slip ratio), the red is Fy (lateral) and the green line is Mz (aligning moment).

When the left and right side traction coefficients are not the same, there are two options of braking control: we may refer to either a lower fraction coefficient or to the higher traction coefficient while producing a braking (or driving) torque control [6]. When we refer to the lower traction coefficient (and corresponding wheel), we call this control Select-Low (SL) control, while in the other case we call it Select-High control.

Numerical models of both controls have been created. Two types of the traction coefficients have been considered:

1. slippery road conditions, where a maximum traction coefficient $\mu_m = 0.1$appears at slip $s_m = 0.2$ and the $\mu_b = 0.05$ at the slip $s_b = 1$ (wheels blocked)
2. good road conditions, where a maximum traction coefficient $\mu_m = 1$appears at slip $s_m = 0.2$ and the $\mu_b = 0.4$ at the slip $s_b = 1$.

Fig. 6 shows an experiment of sudden traction coefficient change from good to slippery at a random, 2.5 seconds of braking. The robot control has been switched to the wheels of the lower traction coefficient (application of the SL method). As the braking torque rising and falling slopes have not been changed, the wheels at the lower μ have been suddenly blocked (s = 1).

Fig. 7 shows similar switch from good road conditions to slippery conditions, however at the moment of this switch the braking torque has been instantly lowered to 0 for 0.01 second. Thanks to this torque change the further braking continued successfully without wheel blocking. The braking torque applied to the left rear and the right rear wheels was the same. The low μ wheels (red graph) have been circulating around its maximum value μ_m =0.2, while the slip of the wheels at the bigger μ circulated around small values of s. The front wheels' torque has been calculated using (9).

Fig. 8 shows a sudden switch from the low traction coefficient to a high one at 2.5 seconds of braking. The higher traction coefficient wheels adjust to the change of traction (application of the SH method), but the low traction wheels become blocked after around 0.5 second. If we adjust the braking torque on both wheels to the significant lower value, the lower traction wheels get blocked after some short time (here after around 6 seconds.

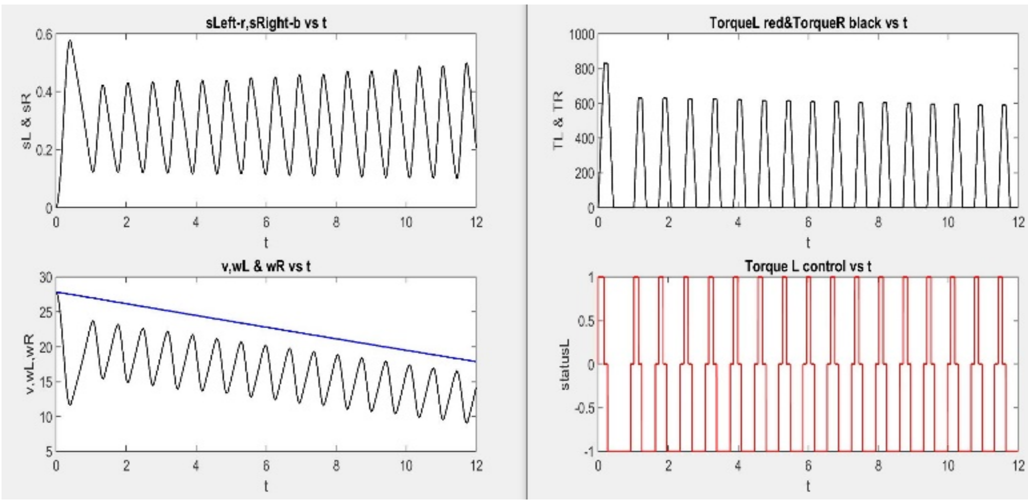

Fig. 6 Symmetric traction c, slippery road conditions

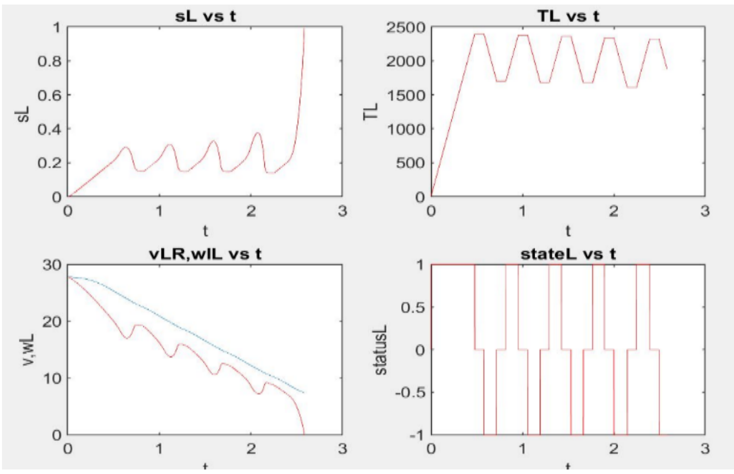

Fig. 7 Symmetric traction c, good road conditions

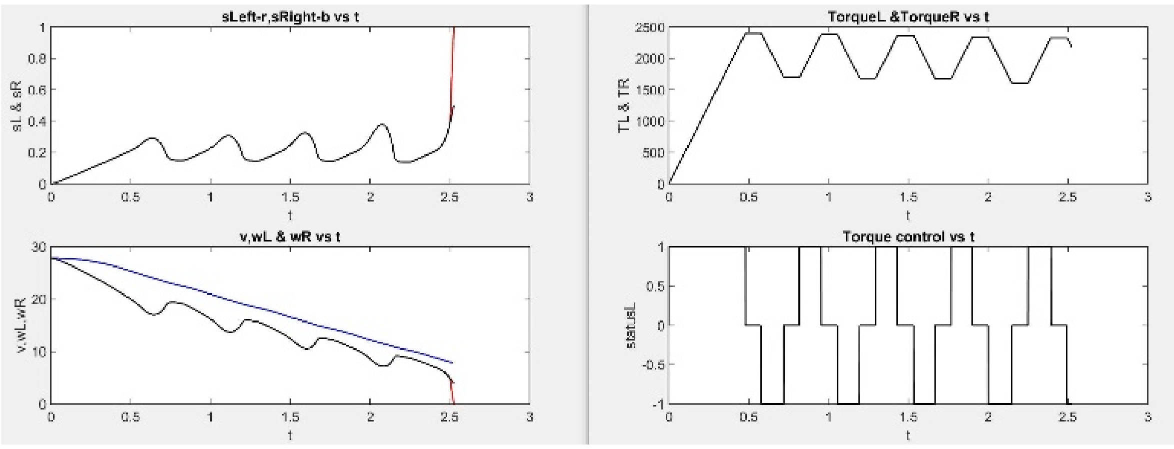

Fig. 8 Switch to SL control no torque adjustment

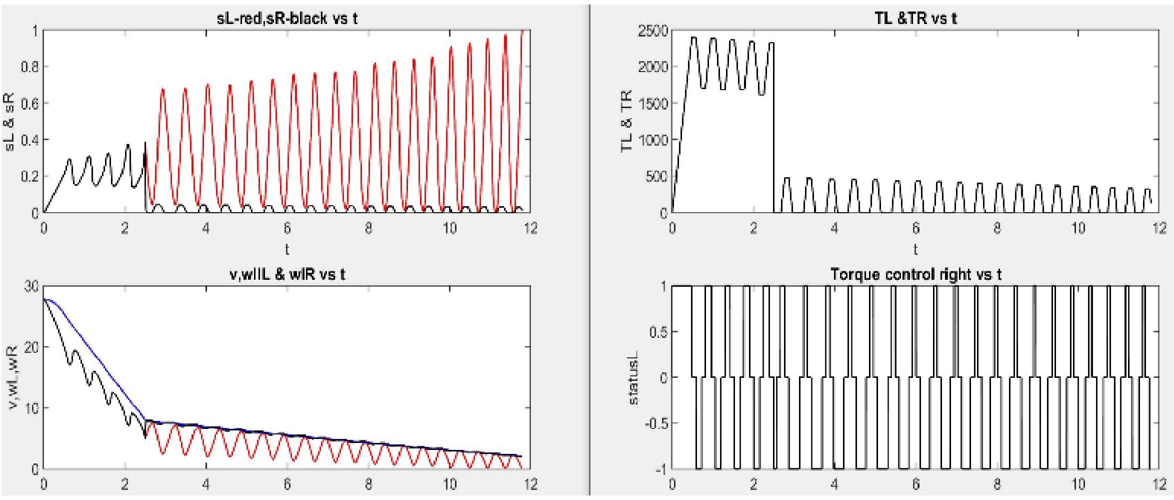

Fig. 9 Switch to SL zeroing torque

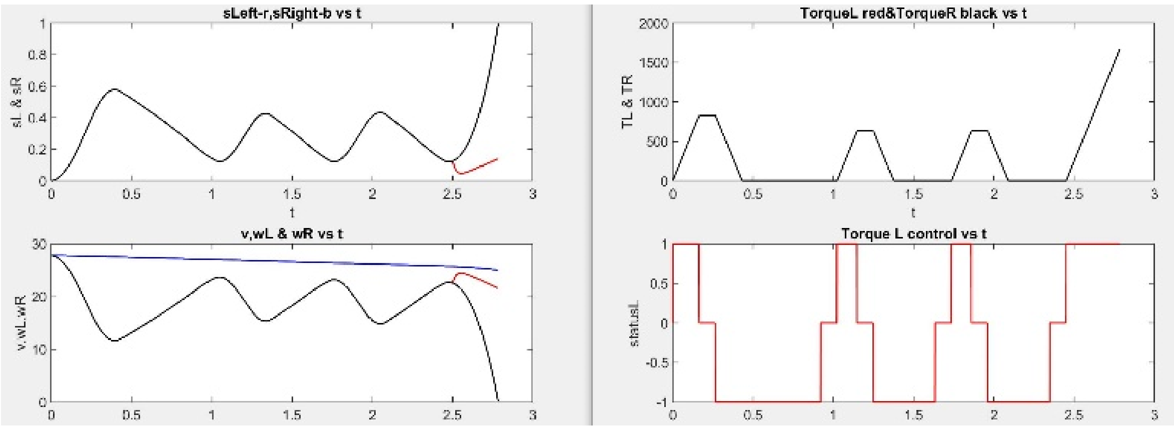

Fig. 10 Switch to SH

On Fig. 9 intermediate lowering the torque to zero (as on Fig. 10) does not help. The wheels still get blocked. The only solution is a significand decrease of a torque slope (from 10k Nm/s to 500 Nm/s) as on Fig. 10.

IV. Conclusion

The SL and SH methods of braking allow for a relatively efficient control of the braking robot. The SL method secures a safe also not very efficient braking. In this method it is important to decrease braking torque in a moment of the switch to the SL. Switch to an SH method may introduce sudden wheel blocks. Especially in the wheel with significantly low traction coefficient. It is possible to avoid the wheels blocking by a dramatic decrease of the braking torque slope.

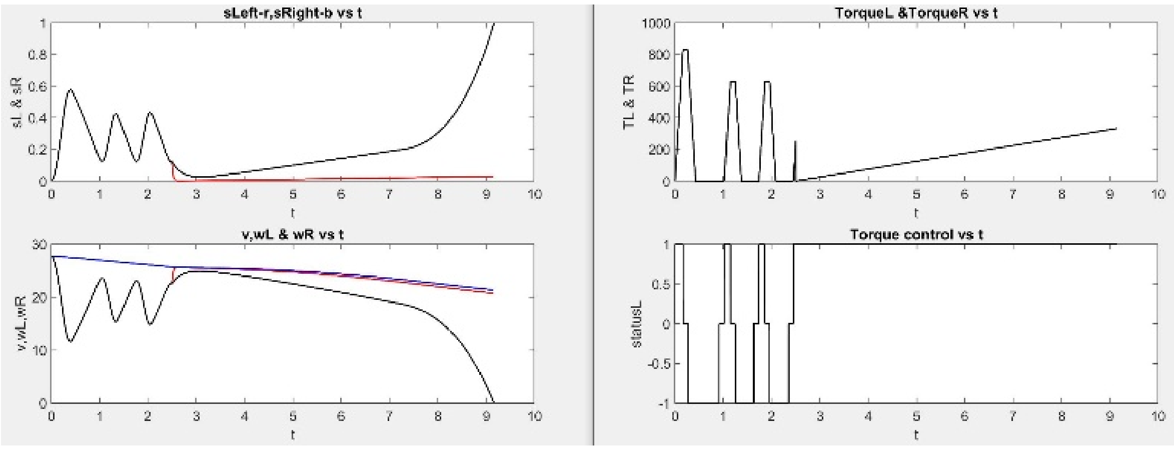

Fig. 11 Switch to SH with torque adjustment

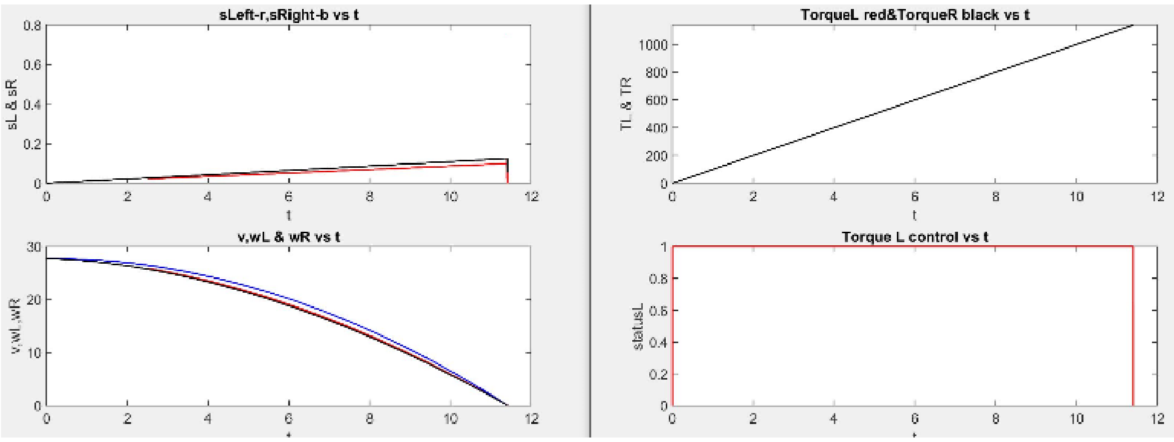

Fig. 12 Switch to SH torque slope decrease

REFERENCES

[1] B.J. Schreyer, „An Inquiry on 2-Mass and Wheeled Mobile Robot Dynamics", ICMARE 2016, 18th International Conference on Mechanical, Automobile and Robotics Conference, Barcelona, Spain, August 11-12, 2016.

[2] B. D. Andrea-Novel, G. Bastin, G. Campion, „Modelling and Control of Non Holonomic Wheeled Moble Robots", Proceedings of the 1991 IEEE, International Conference on Robotics and Automation, Sacramento, California-April 1991, pp1130-1135

[3] C. Samson, K. Ait Abderrahim, „Mobile robot control. Part1: Feedback control of non- holonomic wheeled cart in Cartesian space". Internal report, INRIA, Sophia-Antipolis, France, 1990.

[4] B.J. Schreyer, „Dynamics of braking vehicle", Internal Technical report.

[5] A.Y.Ungoren, H. Peng, and H. E. Tseng, „A study on lateral speed estimation methods,"Int. J. Veh. Auton. Syst., vol. 2, no. 1¡2, pp.126¡144, Jul. 2004.

[6] H. F. Grip, L. Imsland, T. A. Johansen, T. I. Fossen, J. C. Kalkkuhl, and A. Suissa, „Nonlinear vehicle side-slip estimation with friction adaptation, "Automatica", vol. 44, no. 3, pp. 611¡622, Mar. 2008.

[7] http://www.racer.nl/reference/pacejka.htm#:~:text=Some%20interpretations%20for%20the%20Pacejka,apart%20from%20Sh%2C%20Sv).

[8] B. Choi, "Antilock brake system with a continuous wheel slip control to maximize the braking performance and the ride quality," IEEE Transactions on Control Systems Technology, vol. 16, no. 5, pp. 996 – 1003, 2008.

[9] C. Mi, H. Lin, and Y. Zhang, "Iterative learning control of antilock braking of electric and hybrid vehicles," IEEE Transactions on Vehicular Technology, vol. 54, no. 2, pp. 486–494, 2005.

[10] C. Canudas-de Wit and R. Horowitz, "Observers for tire/road contact friction using only wheel angular velocity information," in Proceedings of the IEEE Conference on Decision and Control, vol. 4, Phoenix, AZ, USA, 1999, pp. 3932 – 3937.